Spectral and dynamical effects of octahedral impurities on RE^{3+} in garnets

1998 J. Phys.: Condens. Matter 10 9701

(http://iopscience.iop.org/0953-8984/10/43/013)

J. Phys.: Condens. Matter **10** (1998) 9701–9710. Printed in the UK PII: S0953-8984(98)94933-5

Spectral and dynamical effects of octahedral impurities on RE^{3+} in garnets

A Lupei, V Lupei and E Osiac

Institute of Atomic Physics, Bucharest 76900, Romania

Received 9 June 1998, in final form 26 August 1998

Abstract. The effects of impurity ions that enter octahedral a sites on the spectra of RE^{3+} ions in dodecahedral c sites of garnets are investigated. Two types of such impurities have been studied: nonstoichiometric defects and transition ions (Cr^{3+}). Based on the new data on Er^{3+} in YAG it is shown that a nonstoichiometric defect such as Y^{3+}(a) determines four different perturbations of the nearby Er^{3+}(c) ions (P centres). Due to the low symmetry D_2 at the c site, the four directions of perturbation from the nearby Y^{3+}(a) centres are nonequivalent with respect to the local symmetry axes and determine particular compositions of perturbed crystal fields. If the RE^{3+} ion is a non-Kramers one such as Tm^{3+} or Pr^{3+}, the lowering in symmetry determined by octahedral impurities is clearly observed by additional lines (mainly for one of the P centres) forbidden in D_2. A splitting of $\sim$2 cm^{-1} for one of the P centres in $Er_3Al_5O_{12}$ is assigned to the rise of Kramers degeneracy due to a short-range magnetic order determined by an anisotropic Er^{3+}(c)–Er^{3+}(a) superexchange interaction. Other arguments in favour of anisotropic a–c superexchange interaction are the high energy transfer rates measured for one Er^{3+}(a)–Er^{3+}(c) centre and one Cr^{3+}(a)–Tm^{3+}(c) centre in YAG.

1. Introduction

Garnets doped with rare earth (RE^{3+}) ions represent the most important solid state laser crystals. These crystals offer, in principle, a single site for substitution with three valent RE^{3+} laser active ions, the dodecahedral c site occupied normally with Y^{3+} or Gd^{3+}. Since no charge compensation is necessary for substitution, a unique centre would be expected for the dopant RE^{3+} ions. However, the optical spectra of these ions, especially in the high temperature grown garnet crystals, show a complex multisite structure, some of the additional lines depending on dopant concentration. The investigation of this structure is essential in elucidation of the nature of structural defects. It plays also an important role in the investigation of energy transfer processes which determine the luminescence quenching or up-conversion processes in single or co-doped crystals.

The shifts of RE^{3+} ion energy levels of perturbed centres in garnets with respect to normal ones are determined by changes of local crystal field at the RE^{3+} position determined by other substitutional RE^{3+} or transition ions (or impurities) of different ionic volumes with respect to the replaced ion in the ideal lattice. The perturbing ions can determine modification of symmetry and strength of the crystal field at the RE^{3+} site. In high temperature grown garnets ($Y_3Al_5O_{12}$—YAG—or $Gd_3Ga_5O_{12}$—GGG) four main types of spectral line have been observed in RE^{3+} spectra [1–4]: (i) N lines associated with RE^{3+} in unperturbed dodecahedral c sites of D_2 local symmetry; (ii) lines associated with ensembles of RE^{3+}(c) in nearest neighbour sites such as n.n. RE^{3+}(c) pairs (M lines) or triads (satellites

0953-8984/98/439701+10$19.50

T); (iii) lines A due to RE^{3+} ions in octahedral a-sites of C_{3i} local symmetry; (iv) lines P associated with Y^{3+} (Gd^{3+}) nonstoichiometric defects (an excess of Y^{3+} or Gd^{3+} ions that enter the octahedral sites) or with centres A, placed in the nearest neighbourhood of isolated RE^{3+}(c) or of n.n. ensembles of RE^{3+}(a) ions.

The departure from stoichiometric composition, an excess of Y^{3+} (or Gd^{3+}) that enters the octahedral a sites, is an intrinsic defect of high temperature garnets. This defect, by a different ionic volume, perturbs the crystal field at the RE^{3+}(c) site and leads to the apparition of several P satellites (of almost equal intensity and with relative intensity to N independent of RE^{3+} content for low concentrations) placed asymmetrically around the main lines N. Usually up to three such satellites have been observed leading to the conclusion that three different types of perturbations are produced by Y^{3+}(a) (Gd^{3+}(a)) centres from the first coordination sphere of a dodecahedral c site. An asymmetric distortion of octahedra by substitution with Y^{3+} which makes the six c sites surrounding the octahedron nonequivalent, but preserving the inversion of the a site (three pairs) has been proposed to account for these three P satellites [3], although no explanation for such a distortion was given.

A complex multisite structure is observed also in co-doped crystals either with two RE^{3+} species or with transition ions and RE^{3+}. Though investigated previously, the Cr^{3+}, Tm^{3+} multisite structure in garnets [5–8] has a series of nonelucidated aspects. Since Cr^{3+} enter octahedral sites, the multisite structure determined by codoping for Cr, Tm:YAG should present similarities with that of the nonstoichiometric defect.

In many experiments the global luminescence kinetics of RE^{3+} or co-doped RE^{3+} systems is very complex and presents fast components followed by slower ones, that cannot be explained in terms of conventional theories of energy transfer. This fact has determined a reanalysis (see the review papers [9–13]) of the models concerning the nature of interactions that drive the energy transfer processes between RE^{3+} ions or between transition metal and RE^{3+} ions in crystals. However, sometimes in the proposed models too many parameters are inferred from a given curve. The high resolution spectral and dynamical investigation of shifted lines could give additional information on the nature and strength of the interaction between the dopant ions or inside the ensembles responsible for lineshift. Thus, the type and strength of short range interactions could be inferred.

This paper presents a discussion of the multisite structure of several RE^{3+} ions in the light of new spectral data on Er^{3+} doped YAG and a reanalysis of the structural models of the perturbations leading to multisite structure. Spectral data on various RE^{3+} of different ionic radii such as Pr^{3+}, Nd^{3+}, Er^{3+} or Tm^{3+} are also used in our argumentation. Static (splitting of RE^{3+} Kramers degeneracy) and dynamic effects (fast components in decays) of short range interactions—mainly superexchange—are also presented, based mainly on Er^{3+}:YAG and Cr^{3+},Tm^{3+}:YAG data.

2. Experiment

YAG:Er samples with Er^{3+} content from ∼0.1 at.% to 100 at.% grown by high temperature techniques (Czochralski or Bridgman) have been investigated. The transmission spectra of a cw lamp and the emission under short pulse laser excitation have been measured with a set-up including a computer controlled one meter GDM monochromator, an S_{20} photomultiplier and a multichannel MCS analyser with a resolution of ∼5 ns. The measurements have been performed at different temperatures above 10 K. For excitation of the emission spectra and luminescence kinetics a doubled YAG:Nd laser has been used. Some of the previous data have been obtained by using selective excitation with dye lasers.

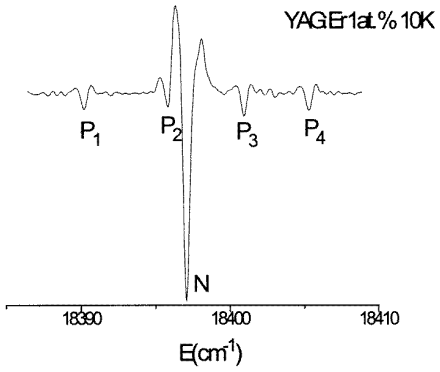

Figure 1. The second derivative of the absorption spectrum of the $^4I_{15/2}(1) \rightarrow {}^4S_{3/2}(1)$ transition in YAG for a sample with 1 at.% Er^{3+} at 10 K.

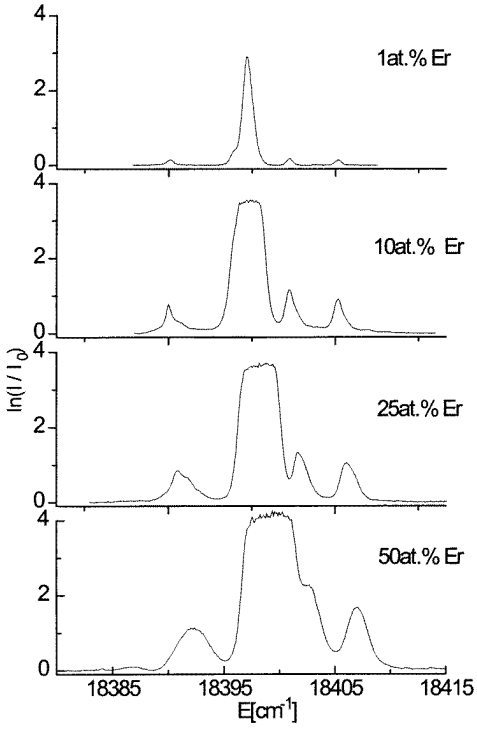

Figure 2. The concentration dependence of the absorption spectrum of the $^4I_{15/2}(1) \rightarrow {}^4S_{3/2}(1)$ Er^{3+} transition in YAG, at 10 K.

3. Results on YAG: Er

3.1. Absorption

We have analysed the high resolution spectra of Er^{3+} in YAG corresponding to the $^4I_{15/2}(1) \leftrightarrow {}^4S_{3/2}(1)$ transition (the crystal levels of Er^{3+} in c sites of D_2 symmetry are Kramers doublets, 1 denoting the first Stark level of the multiplet) in a large concentration range from 0.1 to 100 at.%. The absorption spectra show, besides the Er^{3+} main line N, a multisite structure that changes with Er^{3+} content. Similarities can be observed inside several concentration ranges:

(i) In the low concentration range (up to $\sim$3 at.%), the spectra show besides the main line N four P satellites (instead of three [2] or seven reported previously in the $^4I_{15/2}(1) \rightarrow {}^4I_{13/2}(1)$ transition [3]), of almost equal intensity and with the ratio P/N independent of Er^{3+} content C. The half width of both N and P lines is $\sim$1 cm^{-1}. This structure is better illustrated (figure 1) in the second derivative of the absorption spectrum. The new observed satellite as compared with previous data for the same transition [2] is P_2, situated at ~ -1 cm^{-1} from the main line N. The others satellites are at -7, $+4$, $+8$ cm^{-1} from N.

(ii) In the intermediate concentration range (from about 10 to about 25 at.%), the P_2 satellite is no longer resolved from the N line. Moreover, the main line N and some of the P satellites present on the high energy side additional shoulders, dependent on Er^{3+}

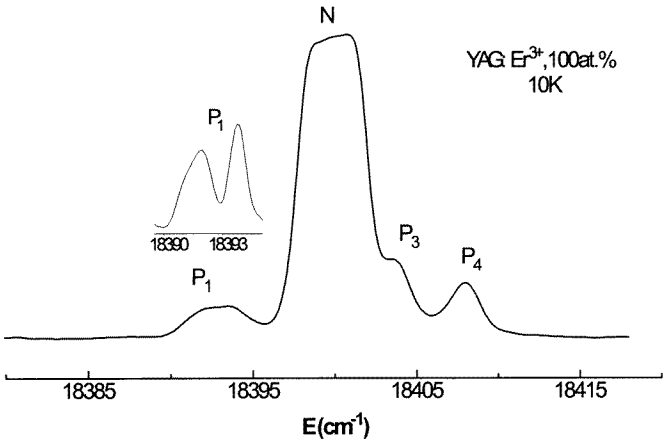

Figure 3. The absorption spectrum of YAG:Er 100 at.% ($^4I_{15/2}(1) \rightarrow {}^4S_{3/2}(1)$ Er^{3+} transition), at 10 K; the insert represents the second derivative of the absorption spectrum in the P_1 region.

concentration. Due to strong absorption we have been able to follow the main line N structure up to ∼10%. An Er^{3+} concentration dependent distortion of the lineshape of the N centre (an unresolved shoulder at $\sim +0.6$ cm^{-1}) is most probably due to a M type line (Er^{3+}(c)–Er^{3+}(c) n.n. pairs). Although this additional structure has been observed in all P resolved satellites, it is more pronounced in the P_1 region where a second line at $\sim +1.2$ cm^{-1}, and a third one at $\sim +2$ cm^{-1}, are resolved. The relative intensity to P_1 of these lines increases with Er^{3+} content (figure 2).

(iii) At higher concentrations the main line and the satellites become broader and the lineshape is more complex, the maximum broadening being at 50 at.%, when the lineshape of satellites are symmetrical; after that it decreases continuously up to 100 at.%. An anisotropic behaviour of P lines broadening is observed. Thus, at 50 at.% P_1 has a linewidth of ∼3.5 cm^{-1}, while that of P_4 is only 2.2 cm^{-1}.

(iv) At 100 at.% the lines present a larger linewidth than that measured at low concentrations. Besides, satellite P_1 presents a clear split in two components separated by ∼2 cm^{-1} (figure 3) while the P_4 linewidth is ∼2 cm^{-1}. The splitting of P_1 is better illustrated in the enclosed detail in figure 3. where the second derivative of the absorption spectrum in the region of the P_1 satellite is presented. This splitting has been observed in all our samples, regardless of the high temperature growth technique.

(v) A monotonic shift of P and N lines with concentration is observed.

3.2. Luminescent emission and decays

The emission spectra and decays have been measured under nonselective pumping with 532 nm, mainly at 10 K. The $^4S_{3/2}$ emission spectra are similar to absorption. The $^4S_{3/2}$ kinetics of each centre is complex and depends on concentration and pumping, suggesting the implication of up-conversion processes too. For this reason the measurements have been performed at very low pumping.

As outlined before [13], at low temperatures the decay of main line N is exponential, but with lifetime depending on concentration, shorter than that of isolated ions (∼17 μs) and suggesting that the supermigration regime has been attained. In this case a transfer rate $W = 1/\tau - 1/\tau_0$ can be defined, where τ is the measured lifetime at a given concentration

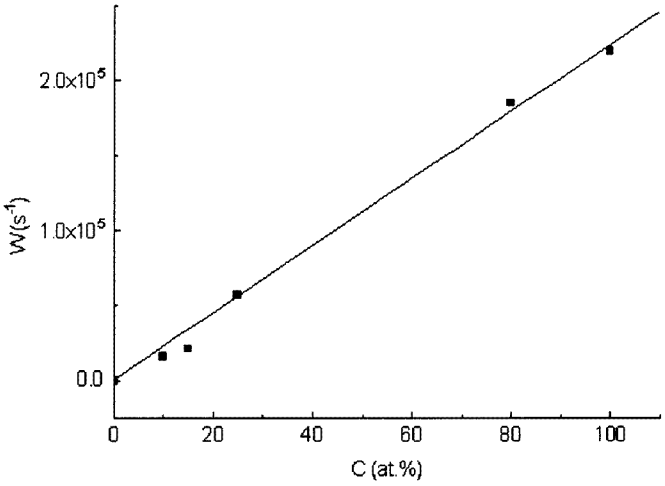

Figure 4. The concentration dependence of the transfer rate for satellite P_4.

and τ_0 is the isolated ion lifetime (measured at 0.1 at.%). The experimental dependence of W on Er^{3+} content is quadratic at high concentrations [13].

At low concentrations the decays of all P lines are, in the limit of experimental errors, exponential too with the same lifetimes as the main line. At higher Er^{3+} content the decays show an anisotropic behaviour. Thus, the decay of P_4 is exponential with a transfer rate W quadratically dependent on concentration at high Er^{3+} content (figure 4) (at 100 at.% the transfer rate is $\sim 2.1\times 10^5\ s^{-1}$), while that of P_1 is more complex with a short nonexponential part followed by a longer exponential part similar to P_4 or N. This is illustrated in figure 5 where the kinetics of the P_1 satellite (figure 5(a)) is compared with that of P_4 (figure 5(b)) for a sample with 100 at.% Er. Though the short part is nonexponential, in the limit of experimental errors, from the slope in origin one could determine a transfer rate of at least $\sim 2.6 \times 10^6\ s^{-1}$.

4. Discussion

4.1. Analysis of Er^{3+}: YAG data

The analysis of Er^{3+}:YAG high resolution $^4I_{15/2}(1) \leftrightarrow S_{3/2}(1)$ absorption, emission and decay characteristics reveals several new facts concerning the Er^{3+} multisite structure in YAG.

(i) The concentration dependence (shift and lineshape) of the main centre N spectra has been analysed in a previous paper by using data on the $^4I_{15}(1) \rightarrow {}^4I_{13}(1)$ Er^{3+} transition [3]. The monotonic shift with increasing Er^{3+} content has been connected to the contraction of the lattice constant from 12.021 Å for YAG to 11.984 Å in EAG and to the change of the line peak structure when passing from very low Er^{3+} concentrations to Er^{3+} only c sites.

In the YAG lattice each c site is surrounded by a co-ordination sphere of four nearest neighbours, of radius 3.7 Å. The first RE^{3+}(c) n.n. ensemble to appear with increasing RE^{3+} concentration is the n.n. pair. The previous studies on such pairs refer to large RE^{3+} ions such as Pr^{3+} or Nd^{3+} [1, 2, 4, 15–17], where the corresponding satellite M is shifted by several (5 to 7) cm^{-1} from line N. The kinetics of M lines for Nd^{3+} $^4F_{3/2}$ or Pr^{3+} $^3P_0$

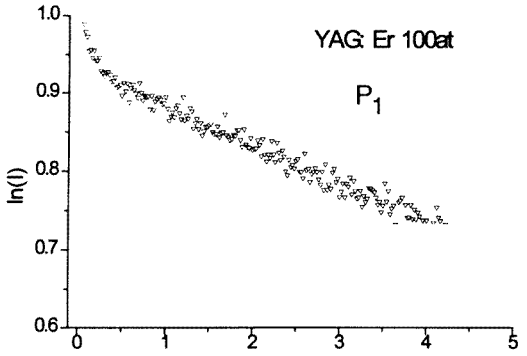

(a)

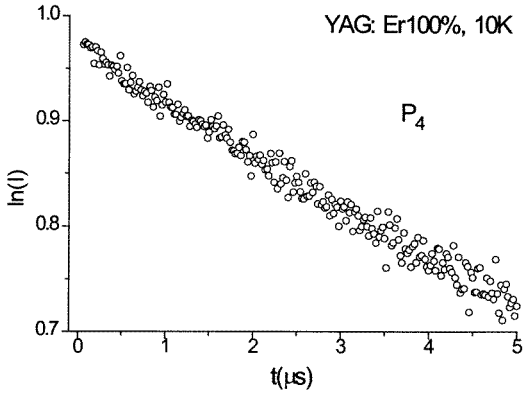

(b)

Figure 5. (a) Time evolution of $^4S_{3/2}$ P_1 emission at 10 K for a YAG:Er 100 at.% sample. (b) Time evolution of $^4S_{3/2}$ P_4 emission at 10 K for a YAG:Er 100 at.% sample.

emission (in YAG or GGG) are strongly quenched, suggesting the presence of a short range interaction—most probably superexchange—between these ions in near neighbour c sites [4, 15–17]. The crystal field distortions inside these ensembles usually do not depend on the direction of distortion and one pair line corresponds to a given coordination sphere. In the case of Er^{3+}:YAG due to the similarity of dodecahedral ionic radii of Er^{3+} and Y^{3+} (1.00 Å and1.02 Å respectively), the mutual distortion inside the n.n. pair is even smaller; a line corresponding to such a pair shows up as an Er^{3+} concentration dependent unresolved shoulder at distance of about 0.6 cm^{-1} from the N line peak on its high energy side in the $^4I_{15/2}(1) \leftrightarrow S_{3/2}(1)$ transition. At higher concentrations, other complex formations of Er^{3+}(c) ions should exist [3]; they could show shifts from the main line, but unfortunately they are not observable in our experiment in the main line. Due to the small shifts of the Er^{3+}(c)–Er^{3+}(c) pair from N we were unable to directly measure the decay of $^4S_{3/2}$ pair lines as in the case of larger RE^{3+} ions.

At 100% Er^{3+} the spectra are given by a unique centre, n.n. quintets (each Er^{3+}(c) is surrounded by four n.n. Er^{3+}(c) ions). The larger linewidth of the N line at 100 at.% as compared with the low concentrations was explained mainly by magnetic dipolar interactions between Er^{3+} in c sites [3]. However, the superexchange interaction between Er^{3+} ions in c sites has been assumed [14] in order to explain the existence of a threshold (at about 15 at.%)

in the concentration dependence of the Curie–Weiss temperature of the antiferromagnetic ordering at very low temperatures ∼1 K.

The data on the $^4S_{3/2}$ main line N emission kinetics (taken with a higher temporal resolution) of Er^{3+} in YAG as function of temperature and concentration confirm the results presented in our previous paper [13]. At l0 K, $^4S_{3/2}$ emission decay (for concentrations larger than ∼3 at.%) is exponential and the quenching could be explained by a dominant migration followed by two-ion and three-ion cross relaxation processes between n.n. Er^{3+} ions; the nature of interaction is most likely dipolar. No short parts in the decays have been observed to confirm the existence of short range interactions between Er^{3+}(c)–Er^{3+}(c).

(ii) At low Er^{3+} concentrations, a clear structure of four satellites (lines P) of equal intensity is seen both in absorption and emission spectra. These lines are associated with a nonstoichiometric defect Y^{3+}(a) (of the high temperature grown garnets) in the first coordination sphere of an Er^{3+}(c) site that contains four a sites. Assuming a random equiprobable distribution of the Y^{3+}(a) centres and that the perturbations do not change the oscillator strengths of the transitions, the estimated concentration of the Y^{3+}(a) centre is about 3% relative to the a sites; this corresponds to the range deduced previously from chemical analyses and optical data [1–4], but not to determinations from EXAFS [18, 19].

Most of the previous studies on RE^{3+} multisite structure in garnets have reported only up to three P satellites, although a few studies revealed more satellites with similar properties, such as the seven-line structure for the transition $^4I_{15}(1) \rightarrow {}^4I_{13}(1)$ of Er^{3+} in YAG [3] or the structure observed for Tb^{3+}, Tm^{3+} in YAG [7, 8, 20]. The three-line P structure was accounted for [3] by a structural model assuming an asymmetric distortion of the O^{2-} octahedron around the a site when substituting Al^{3+} (0.53 Å ionic radius) by Y^{3+} (0.9 Å). Such a distortion could make the six c sites from the first coordination sphere around the a site nonequivalent; however, it was assumed that the Y^{3+}(a) sites still preserve inversion, which would make these six c sites equivalent in pairs. Thus, three non-equivalent pairs of c sites around the Y^{3+}(a) sites are produced and they could induce three different crystal field mutual perturbations at the c sites. A similar effect was assumed in [3] for the c sites from the second sphere around a (Y^{3+}) site in order to account for the other satellites closer to N, observed by Fourier transformed spectroscopy.

However, the garnet lattice does not provide any structural argument why the substituting Y^{3+} ions should produce an asymmetric distortion of the O^{2-} octahedron around the a site. In fact, EXAFS [19] data evidence a dilation of the octahedron with metal–O^{2-} distances changed from 1.937 Å for Al^{3+} to 2.11 Å for Y^{3+}. Thus, the six c sites around the Y^{3+}(a) site continue to be equivalent; however the strong distortion due to substitution of Al^{3+} by Y^{3+} is expected to have important effects on the neighbouring c sites. The first coordination sphere of a sites around a c site contains four positions placed on a tetrahedron. Due to the low symmetry D_2 at the c site, the four directions of perturbation from the Y^{3+}(a) centres are non-equivalent with respect to the local symmetry axes. Therefore, the perturbed crystal fields caused by the four Y(a) sites from the first coordination sphere will not be equal and the spectra should show four P centres. The absence of some of the satellites in the previously analysed spectra is due to their small shift from the unperturbed lines.

With increasing Er^{3+} concentrations, some of these ions could enter the octahedral a sites (A centres [2]), inducing an additional structure of P-like lines. Due to the similarities of the octahedral radii of Y^{3+} and Er^{3+} we were not able to distinguish spectrally the two types of P line structure. However, the lineshape of the P satellites along the range of Er^{3+} concentrations reflects the presence of the various n.n. Er^{3+}(c) ensembles (figure 2); the effect is more pronounced for the P_1 satellite than for P_4, while the satellites P_2 and P_3 cannot be resolved from the main line at high concentrations.

Spectral and kinetic properties of P (Er^{3+}) centres at high Er^{3+} concentrations indicate the existence of superexchange interactions between Er^{3+} ions in c and a sites. At concentrations above ∼80 at.% Er^{3+} the line P_1 is split into two components: the splitting is of about 2 cm^{-1} at 100% Er^{3+}. No such splitting is observed in the other resolved satellite, P_4 (figure 4). This suggests the lifting of Kramers degeneracy by a local magnetic field determined by an exchange interaction between Er^{3+}(c) and Er^{3+}(a) centres. The two line structure could be explained if one assumes that the splitting of the ground Stark level $^4I_{15/2}$ is larger than that of $^4S_{3/2}$; the shoulders observed in figure 4 could be given by the splitting of the upper level. It seems that not only the distance between the a and c Er^{3+} centres (3.35 Å), shorter than that between the n.n. Er^{3+}(c) ions (3.7 Å) is the reason for the larger superexchange interaction. The origin of the splitting of P_1 but not of P_4 is not clear; it might be connected with the anisotropy of the Er^{3+}(c)–Er^{3+}(a) superexchange interaction effect. Such splittings have been observed in optical spectra of Yb^{3+} or Er^{3+} [21–23] in iron garnets, and have been assigned to a short-range order, determined by a superexchange interaction between rare earth ions occupying c sites and Fe^{3+}(a). A splitting of the Cr^{3+} zero-phonon line R1 into two components separated by ∼2 cm^{-1} observed in GGG [24–27] has been assigned to a Cr^{3+}(a)–Gd^{3+}(c) exchange interaction [24, 27].

An anomalous behaviour of P_1 satellite is observed also in the luminescence decays. At 10 K and low concentrations the decays of the satellites P are exponential and their lifetime is similar to that of the main line N. Up to several at.% Er^{3+} the decays become non exponential due to static cross-relaxation processes, then the decays of N and P_4 become again exponential with similar transfer rates depending quadratically on C up to 100% Er. A much faster component shows up at the beginning of the decay of P_1, followed by a slower part, similar to N and P_4. The fast component corresponds to a transfer rate of at least 2.6×10^6 s^{-1}, an order of magnitude larger than for P_4 and it can be induced by a strong short-range interaction. Thus, both the structure and kinetics of satellite P_1 indicates the presence of an anisotropic Er^{3+}(c)–Er^{3+}(a) superexchange.

4.2. Discussion of Cr, Tm: YAG data

It is interesting to compare the anisotropic behaviour of the P-type structure for Er^{3+} in EAG with that of other systems involving the presence of two paramagnetic ions in a and c sites of garnets. Such a system is the well known laser system Cr, Tm:YAG.

We have investigated spectrally the sensitisation of Tm^{3+} emission in YAG with Cr^{3+} ions that occupy the a sites. The mutual influence of the two ions determines the apparition of new satellites in the high resolution spectra of both ions, better resolved in Tm^{3+} spectra. At least three new satellites (C_i) have been separated in Tm^{3+} absorption or emission spectra or in Cr^{3+} excitation spectra [7, 8]. By similarity with P_i satellites, C_i centres could be tentatively assigned to the perturbing effects of Cr^{3+} ions from the first coordination sphere around Tm^{3+}. Though the ionic radius of Cr^{3+} (0.62 Å) is closer to octahedral Al^{3+} (0.53 Å), the distortion produced on the nearby Tm^{3+} is anisotropic. The spectra of two centres, C_1 and C_2, are similar to that of the unperturbed centre N (in the $^3H_4(1) \rightarrow {}^3H_6(1)$ transition the corresponding lines are shifted by -1.1 and respectively $+1.7$ cm^{-1} from N), while for centre C_3 (shifted in the same transition with $+4.6$ cm^{-1} from N) is different. This is illustrated in figure 6 where part of the emission spectra corresponding to the $^3H_4 \rightarrow {}^3H_6$ Tm^{3+} transition for N and C_3 are presented (the notations of [7, 8] for Stark components of $^3H_4$ and $^3H_6$ multiplets are preserved). Tm^{3+} Stark levels in D_2 symmetry are singlets and $\Gamma_i \rightarrow \Gamma_i$ are forbidden transitions, therefore the changes in symmetry and strengths of crystal field should be observed. Indeed, $W_1(\Gamma_1) \rightarrow Z_{2,5}(\Gamma_1)$ forbidden transitions in D_2

are missing from the N spectrum, but they have rather high intensity for C_3 (figure 6). The relative intensity of the other lines is also changed, suggesting a quite different composition of the crystal field Hamiltonian for this centre.

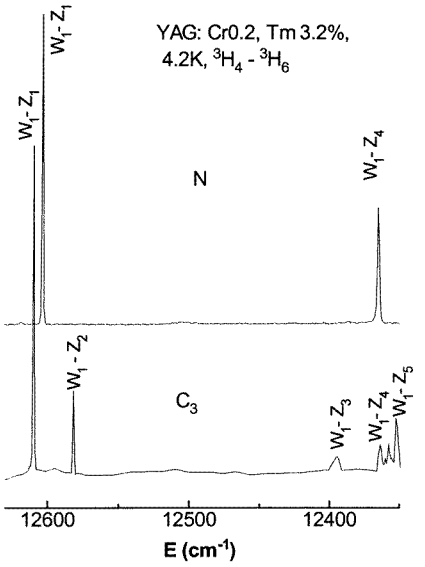

Figure 6. Part of the $^3H_4$ Tm^{3+} emission spectra under selective excitation for a sample of Cr 0.2 at.%, Tm 3.2 at.%: YAG. The upper part corresponds to N centre emission, while the lower one to C_3 Tm^{3+} perturbed centre.

The $^3H_4$ emission decays of these new satellites C_i on pumping in sensitizer (Cr^{3+}) show very large differences: the emission of C_3 centres starts immediately after pumping in Cr^{3+}, regardless of temperature and Tm^{3+} concentration (up to 5 at.%) and the emission decay part is determined by Tm^{3+} de-excitation properties, while for centres C_1 and C_2 the temporal evolution presents decays dependent on these factors. For centre C_3, the Cr^{3+} and Tm^{3+} ions are coupled by a strong short-range interaction (most probably superexchange) of rate $\sim 2.5 \times 10^7$ s^{-1}. The risetime maximum values for centres C_1 and C_2 suggest that they correspond to Cr^{3+}–Tm^{3+} pairs coupled by multipolar interactions; the transfer rate for these centres is relatively slow and thus the emission decay part is determined by the global Cr^{3+} de-excitation processes. A similar situation is observed for N emission.

Therefore, as in the case of Er^{3+} in YAG there is an anisotropic behaviour of Tm^{3+}(c)–Cr^{3+}(a) centres, that is difficult to explain in structural terms. The data on Cr, Tm:YAG show a connection between the distortion and superexchange interaction.

5. Conclusions

It has been demonstrated experimentally that a nonstoichiometric defect of the type Y^{3+}(a) or Gd^{3+}(a) in YAG or GGG due to large differences in ionic radii as compared with host ions leads to four different perturbations of the crystal field at the RE^{3+} occupying dodecahedral c sites, P centres. The first coordination sphere of a sites around a c site contains four positions placed on a tetrahedron. Due to the low symmetry D_2 at the c site, the four directions of perturbation from the Y^{3+}(a) centres are non-equivalent with respect to the local symmetry axes and determine different compositions of perturbed crystal fields. For

non-Kramers RE^{3+} ions, such as Tm^{3+} or Pr^{3+}, the lowering in symmetry for P centres is clearly observed by additional lines forbidden in D_2.

The splitting of RE^{3+} Kramers degeneracy, influenced by short-range magnetic order, could be observed in high-resolution optical experiments if the a sites are occupied by magnetic ions such as Er^{3+} in EAG. Such a splitting has been observed only for one P centre and assigned to anisotropic superexchange interaction Er^{3+}(c)–Er^{3+}(a). A short component in the emission decay of this centre is an additional argument in favour of the presence of superexchange interaction.

The centres induced by Cr^{3+} co-doping in Tm^{3+} spectra in YAG have different spectral and dynamical YAG behaviour. Again one centre presents a larger perturbation of the crystal field and the decay data suggest superexchange interaction between Cr^{3+}(a) and Tm^{3+}(c) for this.

References

[1] Voronko Yu K and Sobol A A 1975 *Phys. Status Solidi* a **27** 257
[2] Osiko V V, Voronko Yu K and Sobol A A 1984 *Crystals 10* (Springer) p 87
[3] Agladze N Y, Bagdasarov H S, Vinogradov E A, Zhekov V I, Murina T M, Popova N N and Fedov E A 1988 *Kristallografia* **33** 913
[4] Lupei V, Lupei A, Tiseanu C, Georgescu S, Stoicescu C and Nanau P M 1995 *Phys. Rev.* B **95** 8
[5] Nie W, Kalinsky Y, Pedrini C, Monteil A and Boulon G 1990 *Opt. Quant. Elect.* **22** S123–S131
[6] Brenier A, Boulon G, Pedrini C and Madej C 1992 *J. Appl. Phys.* **71** 6062
[7] Lupei A, Tiseanu C and Lupei V 1992 *Phys. Rev.* B **47** 14 084
[8] Lupei V, Lou L, Boulon G, Lupei A and Tiseanu C 1993 *J. Physique* I **3** 1245
[9] Barbosa-Garcia O and Struck W 1994 *J. Chem. Phys.* **100** 4554
[10] Basiev T T and Orlovskii Yu V, Privis Yu S 1996 *Solid State Physics* vol 38 (New York: Academic) p 1023
[11] Rotman S R, Luria E, Yitzhaki N and Eyal A 1996 *Opt. Mater.* **5** 1
[12] Lupei V, Lupei A and Boulon G 1996 *Phys. Rev.* B **53** 1
[13] Lupei A, Lupei V, Georgescu S, Ursu I, Jekov V I, Murina T M and Prokhorov A M 1990 *Phys. Rev.* B **41** 10 923
[14] Bagdasarov H S, Dodokin A P and Sorokin A A 1988 *Sov. Solid State Phys.* **30** 1487
[15] Lupei A, Gross H and Reiche P 1995 *J. Phys.: Condens. Matter* **7** 5701
[16] Malinowski M, Szczepanski P, Wolinski W, Wolski R and Frucacz R 1993 *J. Phys.: Condens. Matter* **5** 6469
[17] Lupei A, Lupei V, Osiac E and Petraru A 1998 *Rom. J. Phys.* **43** No 1/2
[18] Jun Dong and Lu Kunquan 1991 *Phys. Rev.* B **43** 8808
[19] Wu Zhonghua, Lu Kunquan, Dong Jun, Li Fenyu, Fu Zhegmin and Fang Zhengzh 1991 *Z. Phys.* B **82** 15
[20] Bayerer R, Heber J and Mateika D 1986 *Z. Phys.* B **64** 201
[21] Wickersheimer K A 1961 *Phys. Rev.* **142** 115
[22] Orlich E and Hufner S 1970 *Z. Phys.* **232** 418
[23] Hufner S 1978 *Optical Spectra of Transparent Rare Earth Compounds* (New York: Academic)
[24] Burns G, Geis A E and Blazey K W 1966 *J. Appl. Phys.* **37** 1301
[25] Struve B and Huber G 1985 *Appl. Phys.* B **36** 195
[26] Monteil A, Nie W, Madej C and Boulon G 1990 *Opt. Quantum Electron.* **22** S247
[27] Yamaga M, Yue Gao, Henderson B and O'Donnell K P 1992 *J. Phys.: Condens. Matter* **4** 7307